Int J Thermophys (2008) 29:1907–1920
DOI 10.1007/s10765-008-0386-0

Polymer Microstructures: Modification and Characterization by Fluid Sorption

S. A. E. Boyer · M. Baba · J.-M. Nedelec · Jean-Pierre E. Grolier

Published online: 5 March 2008

Abstract Polymer micro-organization can be modified by a combination of three constraints, thermal, hydrostatic, and fluid sorption. In selecting the fluid's nature, chemically active or inert, and its physical state, liquid or supercritical, new "materials" can be generated. In addition, the interplay of temperature and pressure allows tailoring the obtained material structure for specific applications. Several complementary techniques have been developed to modify, analyze, and characterize the end products: scanning transitiometry, vibrating-wire (VW)-PVT coupling, thermoporosimetry, and temperature-modulated DSC (TMDSC). The great variety of possible applications in materials science is illustrated with different polymers which can produce materials from soft gel to rigid foams when submitted to fluid sorption, typical fluids being methane or a simple gas (CO_2 or N_2). Absorption of an appropriate fluid in a cross-linked polymer leads to a swelling phenomenon. Thermoporosimetry is a calorimetric technique developed to measure the shift by confinement of thermal-transition temperatures of the swelling fluids, which can be currently used solvents or mercury.

S. A. E. Boyer · M. Baba · J.-P. E. Grolier (✉)
Laboratoire de Thermodynamique des Solutions et des Polymères, Université Blaise Pascal, 24, Avenue des Landais, 63177 Aubiere, France
e-mail: j-pierre.grolier@univ-bpclermont.fr

S. A. E. Boyer
Department of Applied Chemistry, Graduate School of Engineering, Tokyo Metropolitan University, Hachiouji, Tokyo, Japan

Present Address:
S. A. E. Boyer
Centre de Mise en Forme des Matériaux (CEMEF), Ecole Nationale Supérieure des Mines de Paris, 06904 Sophia Antipolis, France

J.-M. Nedelec
Laboratoire des Matériaux Inorganiques, Université Blaise Pascal et Ecole Nationale Supérieure de Chimie de Clermont-Ferrand, 24, Avenue des Landais, 63177 Aubiere, France

Application of thermoporosimetry to a swollen cross-linked polymer allows calculation of the mesh size distribution and evaluation of the degree of reticulation of the polymer. The same technique can be applied to characterize the pore size distribution in a foamed polymer.

Keywords Mesh size distribution · Polymer foam · Pore size distribution · Scanning transitiometry · Temperature-modulated DSC · Thermoporosimetry · Vibrating-wire weight sensor

1 Introduction

Selection of materials is usually made according to their thermophysical properties and their structural characteristics. In numerous industrial applications, in nanoscience at large, making use of advanced nanotechnologies, polymers are playing a major role. Due to their intimate native and their many modified structures, polymers offer a large spectrum of useful all-purpose materials. Among possible tailored polymer structures, most of them are obtained by modifying the polymer micro-organizations through foaming processes. The polymer-foaming sector is certainly one of the most active branches of industrial activity in materials science. Efficient foaming is developed by using selected blowing agents. As a result of the negative impact on the environment of most of the blowing agents traditionally employed up to now, an international regulation has imposed a ban on all chlorofluorohydrocarbon-type blowing agents. Replacement agents, including simple gases like CO_2 or N_2, are currently proposed and exploited [1]. Therefore, ongoing active research is focused on polymer/gas interactions in terms of the energy of interaction and solubility, as well as polymer swelling under gas sorption. As a matter of fact, the micro-organization of polymers can be modified by the combination of three constraints, thermal, hydrostatic, and fluid sorption. In selecting the fluid's nature, chemically active or inert, and its physical state, liquid or supercritical, new "materials" can be generated. Furthermore, the interplay of temperature and pressure allows obtaining material structures in demand for specific applications. In this context, several complementary techniques have been developed to analyze, characterize, and modify the polymers' organization: scanning transitiometry, vibrating-wire (VW)-*PVT* coupling, thermoporosimetry, and temperature modulated DSC (TMDSC). In what follows, the different techniques are shortly described and selected examples are used to illustrate their pertinent contribution.

2 Scanning Transitionometry

The use of state variables (*P, V,* and *T*) in scanning calorimetric measurements has led [2,3] from *PVT* calorimetry to the now well-established scanning transitiometry technique [4]. With this technique the simultaneous determination of thermal and mechanical responses of the investigated system, pertubated by a variation of an independent thermodynamic variable while the other independent variable is kept automatically constant, allows the determination of thermodynamic derivatives over extended ranges of pressure and temperature, impossible to obtain by other known techniques. Four

thermodynamic situations are thus possible to realize in the instruments based on such technique, namely, *PVT*-controlled scanning calorimeters or simply scanning transitiometers, since they are particularly adapted to investigate transitions by scanning one of the three thermodynamic variables. The four possible thermodynamic situations are obtained by simultaneous recording of both heat flow (thermal output) and the change of the dependable variable (mechanical output). Then, making use of the respective related Maxwell relations, one readily obtains the main thermophysical properties as follows: (a) scanning pressure under isothermal conditions yields the isobaric thermal expansivity α_P and the isothermal compressibility κ_T as functions of pressure at a given temperature; (b) scanning volume under isothermal conditions yields the isochoric thermal pressure coefficient β_V and the isothermal compressibility κ_T as functions of volume at a given temperature; (c) scanning temperature under isobaric conditions yields the isobaric heat capacity C_P and the isobaric thermal expansivity α_P as functions of temperature at a given pressure; and (d) scanning temperature under isochoric conditions yields the isochoric heat capacity C_V and the isochoric thermal pressure coefficient β_V as functions of temperature at a given volume.

A detailed description of a basic scanning transitiometer (from BGR TECH, Warsaw, Poland) used in the present applications to polymers is given elsewhere [5]. It consists of a calorimeter equipped with high-pressure vessels, a *PVT* system, and a LabVIEW-based virtual instrument (VI) software. Two cylindrical calorimetric detectors (ext. diameter of 17 mm, length of 80 mm) made from 622 chromel-alumel thermocouples each are mounted differentially and connected to a nanovolt amplifier. The calorimetric detectors are placed in a calorimetric metallic block, the temperature of which is directly controlled with an entirely digital feedback loop of 22-bit resolution ($\sim 10^{-4}$ K), being part of the transitiometer software. The calorimetric block is surrounded by a heating-cooling shield connected to an ultracryostat (Unistat 385 from Huber, Germany), and the temperature difference between the block and the heating-cooling shield is set constant (5, 10, 20, or 30 K) as controlled by an additional analog controller. The whole assembly is placed in a thermally insulated stainless-steel body and placed on a stand, which permits movement of the calorimeter up and down over the calorimetric vessels. The operating ranges of scanning transitiometry are 173 K $< T <$ 673 K and 0.1 MPa $< P <$ 200 MPa (or 400 MPa).

According to its basic principle, a scanning transitiometer can then be operated in different scanning situations. In particular, two main scanning situations, as described in Fig. 1, have been used: pressure-controlled scanning transitiometry (PCST) and temperature-controlled scanning transitiometry (TCST). In addition, the differential mounting of the calorimetric detector permits measurements of the differential heat flux between the reference and the measuring cells, resulting from the physicochemical effects occurring in the investigated systems/phenomena. The advantage of PCST is well illustrated by the study of polymer/gas systems, in particular during sorption (compression by gas-pressurizing fluid)/desorption (by decompression of gas-pressuring fluid) pressure scans. Taking advantage of the respective role of the measuring and reference cells, two modes have been preferably used (as shown in Fig. 2a and b respectively), the thermal differential II comparative in which two different polymers can be directly compared and the thermal differential II in which a polymer sample is characterized versus an inert reference (steel, for example). For each thermal mode,

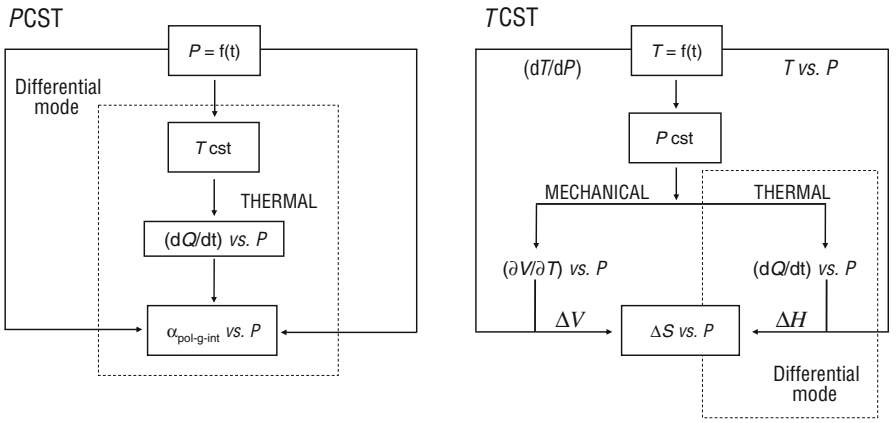

Fig. 1 Schematic view of *PVT*-controlled scanning transitiometry showing two main scanning situations, pressure-controlled scanning transitiometry (*P*CST) and temperature-controlled scanning transitiometry (*T*CST). The *P*CST situation, under isothermal *P*-scans, yields through the thermal output the isobaric thermal expansivity (here $\alpha_{\mathrm{pol-g-int}}$ is for a polymer sample interacting with a gas). The *T*CST situation, under isobaric *T*-scans, yields through combination of both thermal and mechanical outputs the entropy change

the measured heat rate with a polymer was corrected for the heat effects produced by pressurization/depressurization of the hydraulic fluid (expansibility) and the volume sample (asymmetry of the cells). The thermal differential II comparative mode was chosen to directly compare the difference in behavior of two polymers submitted simultaneously to the sorption/desorption of the same gas under the same T and P conditions. For this, samples of identical size and shape of two polymers, medium-density polyethylene (MDPE) and poly(vinylidene fluoride) (PVDF), were placed in the two cells connected to the gas line. Isothermal pressure scans were performed using CO_2 as a pressure transmitting fluid. Measurements were taken on polymers in the solid state, i.e., between glass- and melting-transition temperatures, at different temperatures between 353 K and 403 K, and at each temperature, pressure was scanned up to 100 MPa. The calorimetric signal, that is, the comparative $\{(\mathrm{MDPE}-\mathrm{PVDF})/\mathrm{CO_2}\}$ differential II heat flux is then proportional to the thermal effect due to the difference of the {polymer/gas} interactions between the two polymers. Interestingly, below 40 MPa, the calorimetric signal $\mathrm{d}Q\ \{(\mathrm{MDPE}-\mathrm{PVDF})/\mathrm{CO_2}\}/\mathrm{d}P\ <0\}$ is endothermic; thus, PVDF exhibits larger interactions with CO_2 than does MPDE. Above 40 MPa, the reverse situation is observed, the calorimetric signal $\mathrm{d}Q\ \{(\mathrm{MDPE}-\mathrm{PVDF})/\mathrm{CO_2}\}/\mathrm{d}P\ >0\}$ is exothermic showing that MDPE exhibits larger interactions with CO_2 [6].

The simple thermal differential I mode, as shown in Fig. 2c, where the differential heat flux is measured between the measuring cell containing a polymer sample and the empty reference cell (and not connected to the pressure line) acting only as a thermal reference was used in the temperature-controlled scanning transitiometry (*T*CST) situation. Typically, *T*CST was chosen to investigate transitions and modifications of polymers submitted to isobaric temperature scans. For example, measurements were taken on polymer samples for cooling or heating between 223 and 473 K at different pressures up to 100 MPa. Under such possible $P-T$ conditions, melting/crystallization

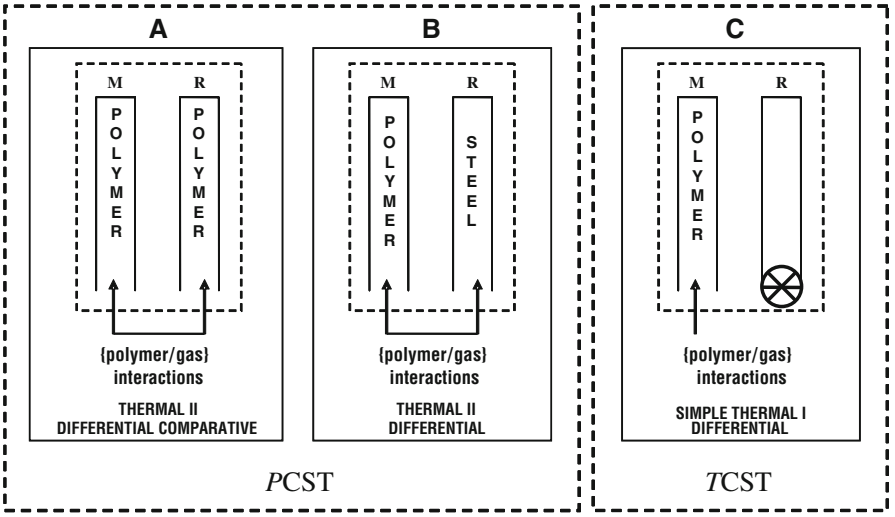

Fig. 2 Schematic representation of *PVT*-controlled scanning transitiometry showing the calorimetric detector housing the twin cells connected to the high-pressure *PVT* line. According to the respective role of the measuring M and reference R cells, three thermal modes are described. In the *P*CST situation: (**a**) the thermal II differential comparative mode, where both measuring and reference cells contain a polymer and are connected to the gas line; (**b**) the thermal II differential mode, where the measuring cell contains the polymer and the reference cell contains an inert sample of equal volume, both cells are connected to the gas line. In the *T*CST situation: (**c**) the simple thermal I differential mode, where the measuring cell contains the polymer and is connected to the gas line while the reference cell acts as a thermal reference

and glass transitions can be fully characterized. The hydraulic fluid can either be a neutral fluid like mercury or a simple gas like carbon dioxide, nitrogen, or methane. In this context, several studies have been successfully conducted, namely, modification of the polystyrene glass transition by high-pressure methane [7], and isobaric thermal expansion of polymers (MDPE, PVDF) in the absence or in the presence of solubilized gases (CO_2, N_2) [1,8]. Another advantage of *T*CST is certainly the possibility, through the rigorous thermodynamic control of the process, to foam polymers. The foam structure (type, size, polydispersity of microcavities) is monitored by controlling both T and P and also the nature of the pressurizing fluid (actually, the hydraulic fluid itself) [9].

Regarding nanoscale self-assembled molecular organization in liquid crystalline-type amphiphilic diblock copolymers, the use of *T*CST is well described [6,10,11] by the systematic investigation of PEO_m–*b*–$PMA(Az)_n$ type polymers (with m and n degrees of polymerization) containing hydrophilic polyethylene oxide (PEO) and hydrophobic azophenyl (PMA(Az)) moieties. Isobaric scans over the isotropic transition of PEO_{114}–*b*–$PMA(Az)_{20}$ using either mercury or supercritical CO_2 as pressurizing fluids demonstrated that "inert" mercury and "chemically active" CO_2 have quite opposite effects on the Clapeyron slope of this transition. That is, a lowering of the transition temperature T_{iso} and a concomitant significant decrease of the transition entropy ΔS_{iso} showed that CO_2 sorption into the polymer is facilitated; therefore, the molecular self-organization at the interface polymer/liquid crystal becomes much easier to yield

nanoscale ordered structure, that is, PEO cylinders organized in a hexagonal structure into the liquid crystal domain, as confirmed by atomic force microscopy analysis [10].

3 Vibrating Wire-*PVT* Coupling

Processing of polymer foams is easily controlled when using blowing agents acting chemically to lower the glass transition (plasticization effect) and physically to promote the foaming process (nucleation effect). As a matter of fact, tailoring of foam structures, that is to say adjusting the type of cells, their sizes and shapes, is possible through a quantitative evaluation of the amount of gas, very often in the supercritical state, absorbed in the polymer and also through a fine tuning of both temperature and pressure during processing (usually extrusion-expansion). When dealing with gas sorption in porous materials [12], that is, investigating gas sorption /desorption phenomena depending on the pore distribution, again the quantitative evaluation of the amount of gas involved has to be made. A double technique has been developed to meet such requirements. This new concept [13] combines two techniques, a vibrating-wire (VW) sensor and a pressure decay *PVT* technique. The VW sensor acts as a force sensor to weigh the material sample during sorption while concomitantly the *PVT* technique is used to quantitatively estimate the corresponding number of moles of gas absorbed. When the sample is a polymer, the buoyancy force exerted by the pressurized fluid on the polymer depends on the swollen volume, ΔV_{pol}, of the polymer due to the gas sorption. In fact, the gas sorption does not always (because of the presence of microvoids or free volume in the polymer structure) induce an increase of volume. In the case the gas absorbed makes the polymer to swell, the buoyancy effect does vary and generates a change in the frequency of the vibrating wire. This frequency change, directly resulting from the change in volume ΔV_{pol}, allows then the evaluation of the swollen volume. The VW sensor consists essentially of a high-pressure cell in which the polymer sample is placed in a holder suspended by a thin tungsten wire (diameter of 25 μm, length of 30 mm) in such a way that the wire is positioned in the middle of a high magnetic field generated by a square magnet placed across the high-pressure cell. Through appropriate electrical circuitry and electronic control, the tungsten wire is activated to vibrate. The period of vibration which can be accurately measured is directly related to the mass of the suspended sample. The pressure decay *PVT* method can be used to calculate the number of moles, n_{sol}, of gas [which is initially kept in a high-pressure calibrated cell] absorbed in the polymer, from the measurement of pressure at its initial value P_{i} when the gas enters the measuring cell and its final value P_{f} after the polymer/gas system has returned to thermodynamic equilibrium. The combined VW-*PVT* apparatus is designed to measure sorption of the gas and the concomitant volume change of the polymer at pressures up to 100 MPa from room temperature to 473 K. The experimental method consists of a series of successive transfers of the gas by connecting the calibrated cell to the equilibrium cell which contains the polymer. The initial, P_{i}, and final, P_{f}, pressures are recorded between each transfer. The detailed methodology and the revisited iterative calculation to simultaneously calculate the solubility together with the volume change of the polymer due to sorption [14,15] use two rigorous working equations.

It was shown that the density ρ of the gas appears as a common term in the two rigorous equations,

$$\rho_{\text{gas}} = \frac{M_{\text{g}}}{RT}\,\frac{P_f}{Z_f} \tag{1}$$

Then, the mass m_{sol} of the gas absorbed in the polymer is related to the change in volume ΔV_{pol} of the polymer using Eq. 2;

$$\Delta m_{\text{sol}}^{(k)} = \rho_{\text{pol}}\,\Delta V_{\text{pol}} + d \tag{2}$$

The term d represents the apparent concentration of gas in the polymer, i.e., when the change in volume, ΔV_{pol}, is zero. The vibrating-wire sensor VW is described with rigorous models yielding a working equation in which all parameters have a physical meaning: the natural frequencies; the volume of the container; and the length, the radius and the density of the wire. The pressure decay technique requires Z, the compression factor of the gas entering the polymer and M_{g}, the molar mass of the dissolved gas. The volume of the polymer sample, V_{pol}, together with its associated change, ΔV_{pol}, and the total mass of dissolved gas, m_{sol}, are the only unknown terms.

The vibrating-wire sensor technique is more precise than the *PVT* method. The technique does not generate cumulative errors like in the case of the *PVT* method, when the successive transfers are performed during an isothermal sorption; in addition, it does not require extensive calibrations. Uncertainties come from the experimentally detected natural angular frequencies of the wire which are reduced with the simultaneous acquisition of the phase angle with the amplitude [15]. The evaluation of the gas concentration data is mainly dependent of the first term of Eq. 2 which contains the density of the gas and the change in volume of the polymer. Then, to unambiguously obtain the apparent solubility of the gas in the polymer and the associated change in volume, the Sanchez-Lacombe equation of state was selected to estimate the change in volume of the polymer at different pressures and temperatures [15].

4 Thermoporosimetry

Since the early work of Thomson [16], it is well established that a fluid confined in the pores of a material exhibits a noticeable shift ΔT of its thermal-transition temperatures. Furthermore, it has been shown that this ΔT shift is directly related to the sizes of the pores, as expressed by their radius R_{p}, in which the fluid is trapped [17–19]. Then a knowledge of the $R_{\text{p}}(\Delta T)$ function allows the determination of the sizes of the pores of a given material simply by measuring ΔT for a selected fluid [20,21]. This method, called thermoporosimetry, becomes essential for the determination of the pore size distribution in porous materials. The experimental technique which is relatively simple consists of measuring the transition (crystallization and allotropic transitions) temperatures of the fluid confined in the pores and of the "free" fluid surrounding the material. Actually, the investigated system is made of the porous material oversaturated by the fluid, and the technique makes use of a sensitive differential scanning calorimeter (DSC). In this context, our original contribution was to use

thermoporosimetry to investigate the microstructure of polymeric materials. In this application, a formal analogy was admitted between the notion of a pore in rigid materials and that of a mesh in swollen polymers.

Nanoporous sol-gel derived silica monoliths were used to "calibrate" the solvents used for thermoporosimetry. Careful control of the aging procedure allowed the production of silica gel matrices with tailored textural properties. A number of solvents including linear alkanes [22], cyclohexane [23], substituted benzene [24], CCl_4 [25, 26], acetone [21], and acetonitrile [27] were tested. Various polymers like polystyrene (PS) [26], ethylene-propylene rubber (EPR) [28], ethylene-propylene-diene-monomer (EPDM) [29,30], polybutadiene, polyisoprene [31], and poly(dimethyl siloxane) (PDMS) [32], cross-linked by UV or gamma irradiation, by heating or aging degradation, were characterized and their mesh size distributions calculated.

To illustrate the use of the thermoporosimetry technique, we choose the cyclohexane/PDMS system. The PDMS sample is cross-linked (by peroxide reaction) and is a heavily silica loaded one (30% w/w); this material is used in electrical insulator devices. Cyclohexane was supplied by Aldrich and used without further purification. Cyclohexane, as shown by DSC (see Fig. 3), exhibits two typical thermal transitions. The cooling from room temperature to $-150°C$ at $-0.7°C \cdot min^{-1}$ shows two mean exothermal transitions. The first one (at 3.47°C and releasing 30.38 $J \cdot g^{-1}$ as specific energy) is the liquid-to-solid normal transition marked by a slight supercooling effect of about 3°C. The second transition takes place at $-88.63°C$ and releases $81 J \cdot g^{-1}$, namely, 2.5 times more than the crystallization. The latter corresponds to the transition from allotropic phase I to allotropic phase II. It is well established that cyclohexane undergoes conformational transitions between the chair and boat isomeric forms. As indicated by X-ray diffraction, the boat isomer proportion is less than 1% at room temperature and smaller at lower temperature [33,34]. Then the phase I-to-phase II transition cannot be assigned to this conformational change. The signal of the I-to-II transition exhibits two peaks expressing the fact that the observed transition proceeds in two steps. When heating from $-150°C$ to room temperature, the DSC plot shows inverse transitions of those recorded during the cooling. The first one represents the II-to-I transition and occurs at $-86.34°C$ with the same specific energy. Unexpectedly, only a single peak is present. At 7.15°C the melting transition occurs while releasing 29.6 $J \cdot g^{-1}$. When cyclohexane is confined inside a porous material or a swollen polymeric gel, its thermal transition temperatures are consequently shifted; thermoporosimetry uses this temperature shift to calculate the pore or mesh size distributions of these divided media. In this context our contribution, as illustrated in what follows, was to extend the thermoporosimetry, in particular, toward soft matter characterization.

Effectively, based on its two thermal transitions, cyclohexane can be used as a thermoporometry probe. Figure 4 shows the DSC exotherms related to confined cyclohexane inside well-known textured four different silica gel samples. The characteristics of the four silica gels are given in Table 1. According to our calibration procedure [24], numerical relationships can be established between the radii of the pores where the cyclohexane undergoes the thermodynamical transitions and the related subsequent temperature depressions. The thermoporosimetry formalism can then be used to calculate the pore or the mesh size distributions (PSD or MSD, respectively), namely, for the liquid-to-solid transition,

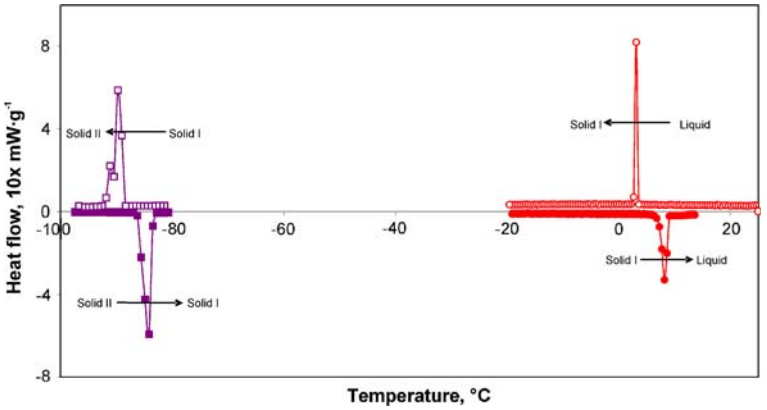

Fig. 3 Thermograms of bulk cyclohexane showing its thermal transitions observed under $0.7°C \cdot min^{-1}$ scanning rate

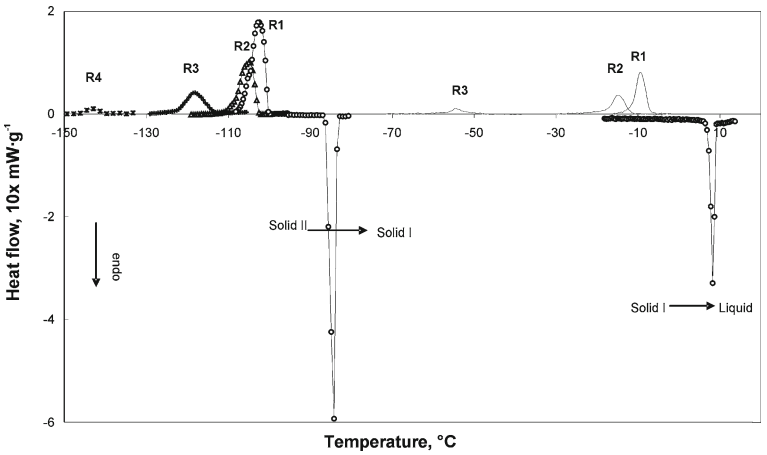

Fig. 4 DSC curves of cyclohexane. The endotherms are related to the bulk cyclohexane, whereas the exotherm signals represent the thermal transitions (liquid to solid I at higher temperatures and solid I to solid II at lower temperatures) of the confined solvent. R1 to R4 are the silica gel samples for calibration described in Table 1. The scanning rate is $0.7°C \cdot min^{-1}$

$$R_p = 2.02 \exp(-\frac{31.99}{\Delta T}) \tag{3}$$

and for the solid-to-solid transition

$$R_p = 1.69 + 12.5 \exp(-\frac{1/\Delta T + 0.075}{0.0205}) \tag{4}$$

where R_p is the radius (in nm) of the pore in which the transition takes place and $\Delta T = T_p - T_0$, the depression temperature. T_p is the temperature in a pore and T_0

Table 1 Textural characteristics of samples used for calibration: SSA, the specific surface area; V_p, the porous volume; R_p, the pore radius; and Max PSD, the maximum of the pore size distribution

Samples	SSA ($m^2 \cdot g^{-1}$)	V_p($cm^3 \cdot g^{-1}$)	R_p (Å)	Max PSD (Å)
R4	532	0.696	26.2	24
R3	473	0.922	39	34.2
R2	166	0.991	119.2	87
R1	183	1.327	144.9	142.5

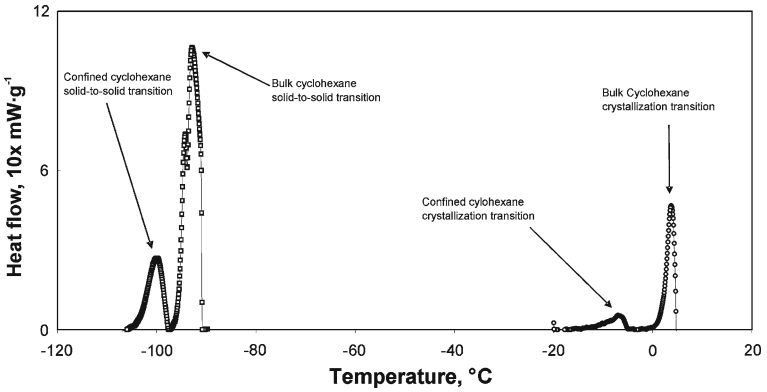

Fig. 5 DSC curves obtained in the case of cyclohexane swelling a PDMS sample. The scanning rate is $0.7°C \cdot min^{-1}$

is the transition temperature of the bulk cyclohexane (7.15°C and −86.34°C for the solid-to-liquid and for the solid-to-solid transitions, respectively).

4.1 Application to Cross-Linked and Filled Polymers

PDMS samples of about 10 mg have been left to swell for 48 h soaking in cyclohexane. A swollen sample was sealed in a DSC aluminum pan and subjected to a cooling temperature program from 10°C down to −115°C with a rate of $0.7°C \cdot min^{-1}$. Figure 5 shows the recorded DSC traces. Two groups of exotherms can be pointed out.

The first group located at high temperature (between 5°C and −20°C) is attributed to the liquid-to-solid transition (crystallization). In this group the first peak is that of the bulk cyclohexane; the second one is attributed to the confined solvent inside the PDMS macromolecular network. The second group of two peaks appearing at lower temperature represents the solid I to solid II transition undergone by cyclohexane. As expected, the first peak is related to the bulk solvent, whereas the second one has to be attributed to the trapped cyclohexane. The solid-to-solid transition, as shown in Figs. 3 and 5, is three times more energetic than the crystallization phenomenon. Peaks of cyclohexane confined in the swollen PDMS sample give a first idea of the mesh size distribution in the polymeric network; however, it was demonstrated that the heat of thermal transition is strongly temperature dependent. Without taking into account this dependence, the smallest pore should be underestimated. Following the calculation

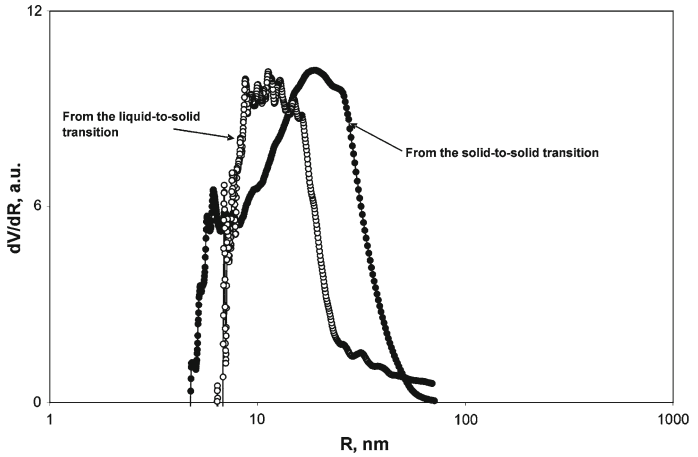

Fig. 6 Mesh size distribution (MSD) of a cross-linked silica loaded PDMS sample swollen by cyclohexane, calculated either from the liquid-to-solid transition or from the solid-to-solid transition, respectively

procedure described elsewhere [23,24], the DSC thermograms can be converted in to the mesh size distributions. Figure 6 shows the mesh size distribution (MSD) of the cross-linked silica filled PDMS sample under study. The data obtained from the liquid-to-solid transition are more scattered than those derived from the solid-to-solid transition, but the satisfactory overlapping of the two distributions has to be noticed. Evidently, the absorbed solvent can be used as a textural probe. Its thermal transitions are highly sensitive to its surrounding constraints. The polymeric meshes of the swollen network limit considerably the degrees of freedom of the cyclohexane molecules leading to a large depression of the phase-transition temperature. Thermoporosimetry appears as a unique tool to investigate cross-linked (insoluble) and filled (opaque) polymers.

5 Temperature-Modulated Differential Scanning Calorimetry (TMDSC)

The rapid evolution of both methodology and technology has led to recent applications of modulated temperature calorimetry, particularly, the combination of the technique with differential scanning calorimetry [35]. Different terms such as "periodic," "oscillating," "dynamic," or "alternating" have thus been used to describe similar techniques based on different types of instruments. The use of temperature-modulated DSC to characterize polymers deals mostly with detection of weak transitions, determination of heat capacities in the quasi-isothermal mode, and separation of superimposed phenomena. The mathematical development necessary to describe the technique is well known [35], and different approaches have been proposed [36]. The total differential heat flow obtained after deconvolution of the modulated heat flow represents the sum of two distinguishable contributions, because the response to the imposed temperature modulation is different depending on the phenomena submitted to the temperature changes. One component, called reversing heat flow, is linked to the heat-

capacity change; the modifications that depend on the temperature scanning rate can be cycled by alternating heating and cooling effects. The second component is linked to the kinetics and is called non-reversing heat flow, by opposition to the first one; modifications appearing in this signal depend only on the temperature.

The specific heat capacity c_p measured with a conventional DSC, under the conditions of negligible temperature gradient within the sample, is approximately proportional to the temperature difference between the sample and the reference or to the heat flow difference. Calculation of the sample heat capacity is possible through calibration data, at the working temperature, via the following relation (m and $m_{Al_2O_3}$ are the mass of the sample and the mass of sapphire used as a standard calibrating substance, respectively):

$$mc_p = m_{Al_2O_3} c_{p(Al_2O_3)} \frac{a_s - a_b}{a_c - a_b} \tag{5}$$

where the quantities a represent the amplitudes of the heat flow (or temperature) difference signals for different situations corresponding to : sample, calibration, and baseline runs designated by s, c, and b, respectively. Usually, the baseline run (a_b) is obtained with two empty aluminum pans. In a measuring run (a_s), the sample is in one of the aluminum pans, whereas in the calibration run (a_c) the sample is replaced by the standard sapphire (Al_2O_3), having a well-known specific heat capacity. In the case of TMDSC, the calibration equation takes the form,

$$(C_s - C_r) = \frac{A_\Delta}{A_{Ts}} \sqrt{\left(\frac{K}{\omega}\right)^2 + C_{r^2}} \tag{6}$$

where C_s and C_r represent the heat capacities of the sample and of the reference, respectively (these quantities include the contributions of the sample and of the pans which can be regarded as identical on the two sides), A_Δ is the temperature difference amplitude between the sample and reference, A_{Ts} is the sample temperature amplitude (in K), and ω designates the modulation frequency ($= 2\pi/p$ with p being the modulation period in s). K is the temperature-dependent Newton's law constant. When calibrating with sapphire, Eq. 7 leads to the following equation:

$$(C_s - C_r) = K_{Cp} \frac{A_{HF}}{\omega A_{Ts}} \tag{7}$$

where A_{HF} refers to the amplitude of the differential heat flow and K_{Cp} is the calibration constant for heat-capacity measurements. The heat capacity of the sample obtained using Eq. 7 allows the determination of the contributions of the reversing and of the non-reversing heat flows noted as HF_{rev} and $HF_{non-rev}$, respectively, to the total heat flow HF_{tot}*using* the following relations:

HF_{rev} signal = average temperature scanning rate × heat capacity signal (conventionally, on heating, a negative sign is necessary because an endothermic effect in the sample, i.e., heat consumption, creates a negative ΔT between the sample and the reference); then, $HF_{non-rev}$ signal = HF_{tot} signal − HF_{rev} signal.

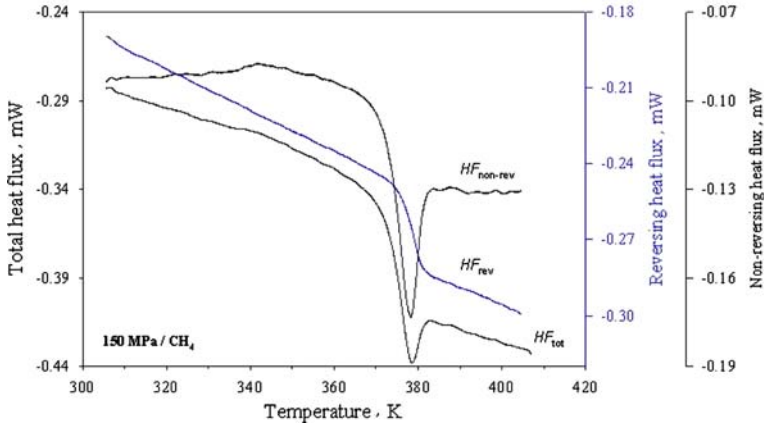

Fig. 7 Thermograms obtained at atmospheric pressure with temperature-modulated differential calorimetry for a polystyrene sample modified by sorption of methane under high pressure (150 MPa). The TMDSC experimental conditions were: amplitude of T, 0.5 K; modulation period, 60 s; scanning rate, $2\,\mathrm{K}\cdot\mathrm{min}^{-1}$. The reversing heat flux HF_{rev} shows clearly the glass-transition inflexion curve which is otherwise hidden in the main fusion peak of the total heat flux HF_{tot}

One of the major advantages of the technique described above is most probably the possibility to access directly in a single-run overlapping effects. In this respect, temperature-modulated DSC appears to be a more powerful technique than standard DSC. The thermal analyzer used in the present work was a Mettler DSC 821 equipped with a refrigeration cooling system, RP 100 (from LabPlant, UK) with a range from 200 K to 700 K. Taking as an example a polystyrene sample modified by high-pressure methane, Fig. 7 illustrates the high potential of the technique to detect unambiguously polymer glass transitions. In Fig. 7 the glass transition clearly appears in the HF_{rev} signal, whereas the HF_{tot} signal does not allow detecting the typical inflexion reflecting the glass transition which is hidden in the main fusion peak.

6 Conclusion

To modify and characterize polymer microstructures, several techniques relevant to rigorous thermodynamics have been recently developed. Calorimetric techniques, particularly *PVT* calorimetry, or scanning transitiometry, and temperature-modulated differential scanning calorimetry, allow through temperature (or pressure) scans to either modify the polymers' micro-organization or to investigate the various transitions undergone by the materials. In addition to the role played by the two variables P and T, a fluid either gaseous (often in supercritical state) or liquid can be advantageously used to promote and/or characterize the polymer nano/microstructure. A complementary technique which combines a weighing technique and a pressure decay *PVT* technique allows evaluation of the amount of gas penetrating a polymer sample or a porous material during sorption under precise control of the different parameters.

References

1. S.A.E. Boyer, M.-H. Klopffer, J. Martin, J.-P.E. Grolier, J. Appl. Polym. Sci. **103**, 1706 (2007)
2. S.L. Randzio, Pure Appl. Chem. **63**, 1409 (1991)
3. S.L. Randzio, J.-P.E. Grolier, J.R. Quint, Rev. Sci. Instrum. **65**, 960 (1994)
4. S.L. Randzio, J.-P.E. Grolier, J. Zaslona, J.R. Quint, French Patent 91-09227, Polish Patent P-295285
5. S.L. Randzio, Ch. Stachowiak, J.-P. E. Grolier, J. Chem. Thermodyn. **35**, 639 (2003)
6. S.A.E. Boyer, Netsu Sokutei **33**, 114 (2006)
7. M. Ribeiro, L. Pison, J.-P.E. Grolier, Polymer **42**, 1653 (2001)
8. S.A.E. Boyer, S.L. Randzio, J.-P.E. Grolier, J. Polym. Sci. Part B Polym. Phys. **44**, 185 (2006)
9. S. Hilic, Ph. D. Thesis, (Blaise Pascal University, Aubière, France, 2000)
10. S.A.E. Boyer, J.-P.E. Grolier, L. Pison, C. Iwamoto, H. Yoshida, T. Iyoda, J. Therm. Anal. Calorim. **85**, 699 (2006)
11. S.A.E. Boyer, J.-P.E. Grolier, H. Yoshida, T. Iyoda, J. Polym. Sci. B Polym. Phys. **45**, 1354 (2007)
12. L. Coiffard, J.-P.E. Grolier, V. Eroshenko, AIChE J. **51**, 1246 (2005)
13. S. Hilic, A.A.H. Padua, J.-P.E. Grolier, Rev. Sci. Instrum. **71**, 4236 (2000)
14. S. Hilic, S.A.E Boyer, A.A.H. Padua, J.-P.E. Grolier, J. Polym. Sci. Part B Polym. Phys. **39**, 2063 (2001)
15. S.A.E. Boyer, J.-P.E. Grolier, Polymer **46**, 3737 (2005)
16. W. Thomson, Phil. Mag. **42**, 448 (1871)
17. W.A. Patrick, W.A. Kemper, J. Phys. Chem. **42**, 369 (1937)
18. C.L. Jackson, G.B. McKenna, J. Chem. Phys. **93**, 9002 (1990)
19. C.L. Jackson, G.B. McKenna, Rubber Chem. Technol. **64**, 760 (1991)
20. M. Brun, A. Lallemand, J.-F. Quinson, C. Eyraud, Thermochim. Acta **21**, 59 (1977)
21. J.-M. Nedelec, J.-P.E. Grolier, M. Baba, J. Sol-Gel Sci. Technol. **40**, 191 (2006)
22. N. Bahloul, M. Baba, J.-M. Nedelec, J. Phys. Chem. B **109**, 16227 (2005)
23. M. Baba, J.-M. Nedelec, J. Lacoste, J.-L. Gardette, J. Non-Cryst. Solids **315**, 228 (2003)
24. N. Billamboz, M. Baba, M. Grivet, J.-M. Nedelec, J. Phys. Chem. B **108**, 12032 (2004)
25. T. Takei, Y. Ooda, M. Fuji, T. Watanabe, M. Chikazawa, Thermochim. Acta **352–353**, 199 (2000)
26. B. Husár, S. Commereuc, L. Lukáč, S. Chmela, J.-M. Nedelec, M. Baba, J. Phys. Chem. B **110**, 5315 (2006)
27. M. Wulff, Thermochim. Acta **419**, 291 (2004)
28. N. Billamboz, J.-M. Nedelec, M. Grivet, M. Baba, Chem. Phys. Chem. **6**, 1126 (2005)
29. M. Baba, J.-M. Nedelec, J. Lacoste, J.L. Gardette, M. Morel, Polym. Degrad. Stabil. **80**, 305 (2003)
30. J.-M. Nedelec, M. Baba, J. Sol-Gel Sci. Technol. **31**, 169 (2004)
31. P.-O. Bussiere, M. Baba, J.-L. Gardette, J. Lacoste. Polym. Degrad. Stabil. **88**, 182 (2005)
32. F. Virlogeux, D. Bianchini, F. Delor-Jestin, M. Baba, J. Lacoste, Polym. Int. **53**, 163 (2004)
33. G.J. Kabo, A.A. Kozyro, M. Frenkel, A.V. Blokhin, Mol. Cryst. Liq. Cryst. **326**, 333 (1999)
34. Y. Shao, G. Hoang, T.W. Zerda, J. Non-Cryst. Solids **182**, 309 (1995)
35. M. Reading, D. Elliot, V.L. Hill, J. Therm. Anal. **40**, 949 (1993)
36. J.E.K. Schawe, Thermochim. Acta **261**, 183 (1995)